

Design, fabrication and characterization of infrared LVOFs for measuring gas composition

This content has been downloaded from IOPscience. Please scroll down to see the full text.

2014 J. Micromech. Microeng. 24 084001

(<http://iopscience.iop.org/0960-1317/24/8/084001>)

View [the table of contents for this issue](#), or go to the [journal homepage](#) for more

Download details:

IP Address: 193.136.13.15

This content was downloaded on 18/09/2014 at 14:20

Please note that [terms and conditions apply](#).

Design, fabrication and characterization of infrared LVOFs for measuring gas composition

M Ghaderi¹, N P Ayerden¹, A Emadi^{1,2}, P Enoksson³, J H Correia⁴,
G de Graaf¹ and R F Wolffenbuttel¹

¹ Electronic Instrumentation, Microelectronics Department, Faculty of EEMCS, Delft University of Technology, Mekelweg 4, 2628 CD, Delft, Netherlands

² Maxim Integrated, 160 Rio Robles, San Jose, CA 95134, USA

³ Micro and Nanosystems, MC2, Chalmers University of Technology, SE412 96, Gothenborg, Sweden

⁴ Department of Industrial Electronics, University of Minho, Campus Azurem, 4800-058 Guimarães, Portugal

E-mail: m.ghaderi@tudelft.nl

Received 2 December 2013, revised 17 February 2014

Accepted for publication 4 March 2014

Published 22 July 2014

Abstract

This paper presents the design, fabrication and characterization of a linear-variable optical-filter (LVOF) that will be used in a micro-spectrometer operating in infrared (IR) for natural gas composition measurement. An LVOF is placed on top of an array of detectors and transforms the optical spectrum into a lateral intensity profile, which is recorded by the detectors. The IR LVOF was fabricated in an IC-compatible process using a photoresist reflow technique, followed by transfer etching of the photoresist into the optical resonator layer. The spectral range between 3 to 5 μm contains the absorption peaks for hydrocarbons, carbon-monoxide and carbon-dioxide. The resulting optical absorption is utilized to measure the gas concentrations in a sample volume. Two LVOF structures were designed and fabricated on silicon wafers using alternate layers of sputtered silicon and silicon-dioxide as the high- and low- refractive index materials. These filters consist of a Fabry–Pérot resonator combined with a band-pass filter designed to block out-of-band transmissions. Finally, the filters were fully characterized with an FTIR spectrometer and showed satisfactory agreement with the optical thin-film simulations. The characterization showed a spectral resolution of 100 nm, which can be further improved with signal processing algorithms. This method makes it possible to fabricate small and robust LVOFs with high resolving power in the IR spectral range directly on the detector array chip.

Keywords: LVOF, micro-spectrometer, hydrocarbon measurement, IC-compatible, optical filter, infrared spectrum

(Some figures may appear in colour only in the online journal)

1. Introduction

The increased global consumption of natural gas as an essential source of energy leads to depletion of natural gas sources. In the Netherlands, the diminished supply of local gas sources has prompted a transition from the extensive use of local gas, the Groningen gas, to a more varied energy source, which is called

‘new gas’ [1, 2]. The new gas consists of imported gas from the Middle East (such as LNG) and newer gas sources like biogas and coal gasification gas mixed with the local gas (table 1). The constant composition of the Groningen gas has been an advantage in burner design, since a fixed setting was sufficient to ensure safe and clean combustion. The new gas comes from a variety of sources; therefore, the end user receives a gas of

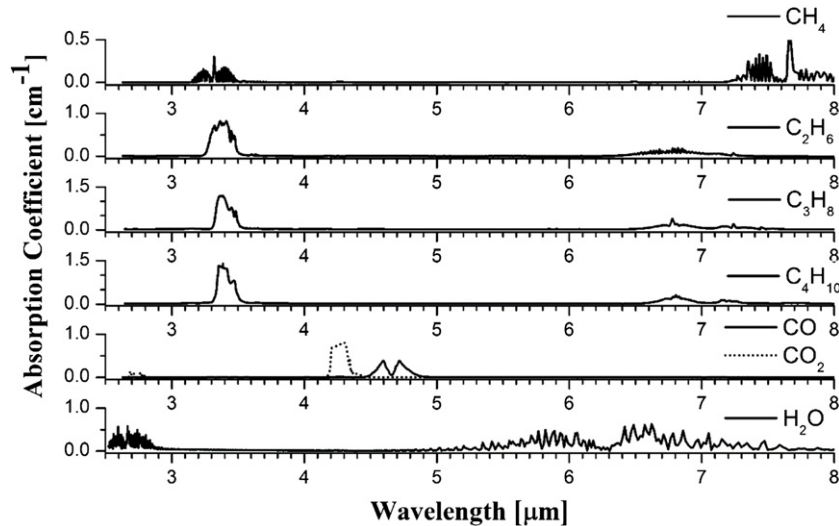


Figure 1. Spectral absorption lines of gases that are relevant in combustion processes [24].

Table 1. Typical combustible gas compositions taken from [2].

	CH ₄ (%)	C _x H _{2x+2} (%)	CO (%)	CO ₂ (%)	N ₂ (%)	H ₂ (%)
Groningen-gas	81	2	–	1	14	–
LNG	87	12	–	–	1	–
Gasification of biomass	12	2	32	23	2	29
Gasification of coal	–	–	4	5	9	81

diverse composition and thus with an unknown energy content. Hence, the composition of the gas fed into the burner needs to be known, and this requires reliable and low-cost gas sensors.

Traditionally, gas composition measurements are performed with expensive industrial gas analyzers, such as gas chromatographs (e.g. [3–5]), or low cost pellistors (e.g. [6, 7]), and electrochemical sensors (e.g. [8, 9]). Compared to pellistors and electrochemical sensors, industrial gas analyzers have a superior detection accuracy; however, they are bulky and not suitable for real-time and *in situ* measurements. While pellistors are small and low-cost sensors, they suffer from signal drift at low (ppm) gas concentrations. Electrochemical sensors also have low selectivity, and the sensitive element is inhibited or degraded by certain chemicals (sensor poisoning) [9]. Over the past few decades, the possibility of fabricating inexpensive sensors using different detection techniques such as optical, viscosity and thermal conductivity sensing has been investigated (e.g. [2, 10–15]). Compared to the other techniques, optical absorption sensing offers attractive features, such as faster acquisition time, lower signal drift, higher reliability and longer lifetime. Furthermore, optical spectroscopy is non-invasive and self-referenced, and it can be used for *in situ* gas detection (e.g. [11, 16–20]).

Most of the gaseous components present in natural gas have absorption spectra located in the 1000–5000 nm spectral range (figure 1). In absorption spectroscopy, these infrared (IR) spectral absorption signatures are used to identify the target gases. While several miniaturized optical gas sensors have been built, these are not fully CMOS compatible, and are also too expensive for the high-volume production that is required for the application in gas distribution [11]. Therefore,

a robust, low-cost, CMOS-compatible and fully integrated MEMS device is needed.

In this paper, we present the design, fabrication and characterization of an infrared linear-variable-optical-filter (LVOF) that will be used in a micro-spectrometer for natural gas analysis. An LVOF-based micro-spectrometer is a tapered-cavity Fabry–Pérot (FP) filter that is placed on top of a linear array of detectors. The LVOF filter transforms the optical spectrum into a lateral intensity profile, which is then recorded by the detectors. This micro-spectrometer was fabricated through a fully controlled CMOS-compatible process and thus it can be integrated into a multi-sensor chip design. The same concept can also be implemented for any wavelength range from UV to IR by choosing the right material combination and optical design. The use of LVOF micro-spectrometers for UV and visible spectral range has already been studied in earlier works [21–23]. This paper applies this method in the infrared to analyze natural gas. The first part of the paper presents the design of the micro-spectrometer. Then, the fabrication flow is explained in the second section. The characterization setup is described and the experimental results are shown in the third section.

2. The system-level optical design

Most of the natural gases have specific optical absorption signatures, usually in the infrared range. Therefore, when it passes through (the length of) a gas cell, a beam of wideband light, generally from a thin-film emitter, is spectrally absorbed according to the gas-specific peaks. Measuring the missing

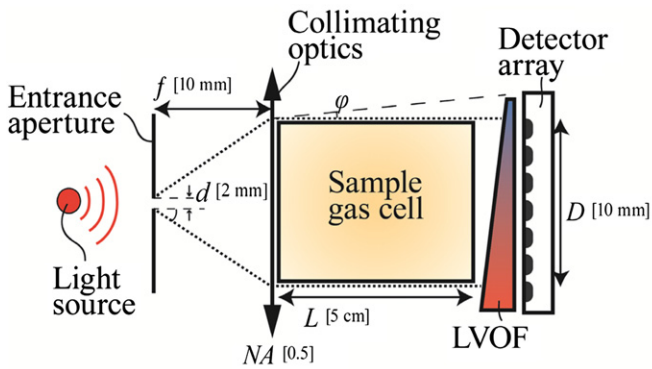


Figure 2. Basic LVOF micro-spectrometer configuration for gas sensing application. The values in brackets are some typical values; the final design might have a different configuration.

wavelengths in the beam reveals the concentrations of the components present in the gas cell. This physical property of the gases is commonly used in optical gas sensors to detect and measure the concentration of target gases. An optical gas sensor is made of three basic elements: a light source, a gas cell and the spectrometer (figure 2). The spectrometer analyzes the spectrum intensity of the light after passing through the gas-cell and reveals the presence and the concentration level of gases in the sample volume. Furthermore, measuring the spectrum without any gas in the chamber can be used as a reference, making this method self-referenced [25].

The optical design of the proposed LVOF-based micro-spectrometer consists of a light source, an aperture, a collimating lens and an LVOF. After passing through the aperture and the lens, the collimated light illuminates the surface of an LVOF (figure 2). The LVOF is a FP type filter and consists of two dielectric multi-layered Bragg reflectors, one on each side of a central resonator cavity layer. The thickness of the cavity layer changes linearly along the length of the filter and determines the wavelength of the transmitted light. Therefore, instead of a large number of discrete filters, which is difficult to fabricate, the LVOF operates as a one-dimensional array of FP filters. By passing through the filter, the light is band-pass filtered according to the width of the resonator at each point and thus by the spatial position along the length of the LVOF [21, 23]. Finally, a detector array positioned underneath the LVOF records the transmitted light. In this way, each detector receives a specific wavelength, and hence the whole structure operates as a micro-spectrometer.

The LVOF is the wavelength-sensitive element in this micro-spectrometer design and should be optically designed to cover the target spectrum. In order to design such a filter, the absorption spectrum of the target gas components should be investigated. Figure 1 depicts the relevant and useable absorption peaks in the wideband infrared absorption spectrum for various components in the combustible gas, spanning the wavelength region from near to mid infrared [24]. Absorption due to water presence is dominant in the infrared, except for the 3–5 μm wavelength range. Therefore, 3–5 μm band is convenient for measuring the gas concentration in the presence of water vapor, resulting in a reliable measurement. In this study, we focus on the range between 3 to 4 μm , in which

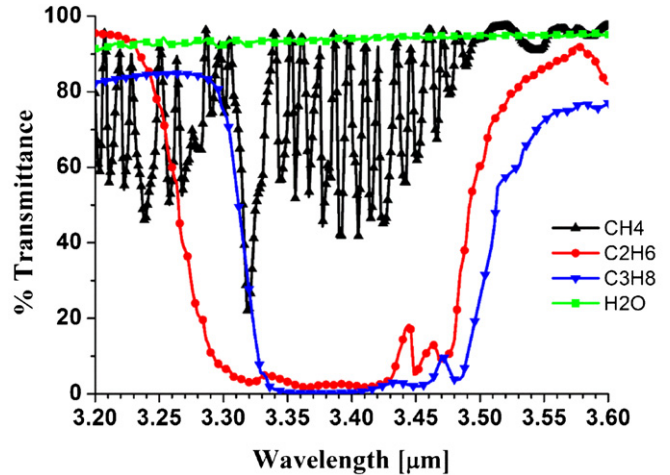


Figure 3. Transmission spectra through a 5 cm gas cell containing different hydrocarbons and water vapor measured at 150 mmHg.

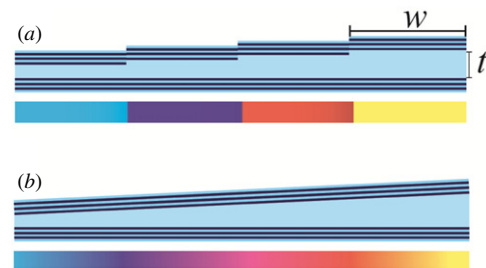


Figure 4. Principle of operation: (a) an array of fixed Fabry-Pérot filters and (b) an LVOF.

the highest peaks for the hydrocarbons are located. A similar approach can also be used for the 4–5 μm band for measuring CO and CO₂.

A closer look into the infrared spectra (figure 3) shows that the absorption peaks of hydrocarbons overlap. Therefore, the absorption at a single wavelength is not directly proportional to the concentration of one component. This complication requires a certain number of measurements performed at different wavelengths, or spectral channels, to obtain the expected accuracy (resolution) on the concentration of the gases. Figure 3, suggests that a minimum spectral resolution of about 10 nm, which is equivalent to a resolving power of about 40 channels over the 3.2 to 3.6 μm spectrum, is sufficient to de-convolve the recorded absorption into gas-specific signatures. This spectral information allows us to measure the concentration of different gases in the sample.

3. LVOF design

This paper investigates an IC-compatible fabrication process for IR LVOFs. Figure 4(a) depicts a one-dimensional array of discrete FP filters with a width of w , and a cavity thickness of t . An LVOF is an array of infinitely many ($w \rightarrow 0$) discrete FP filters, each with a slightly different cavity thickness (t), due to its continuously tapered structure as shown in figure 4(b). The spacing between the mirrors (t) in a FP resonator determines

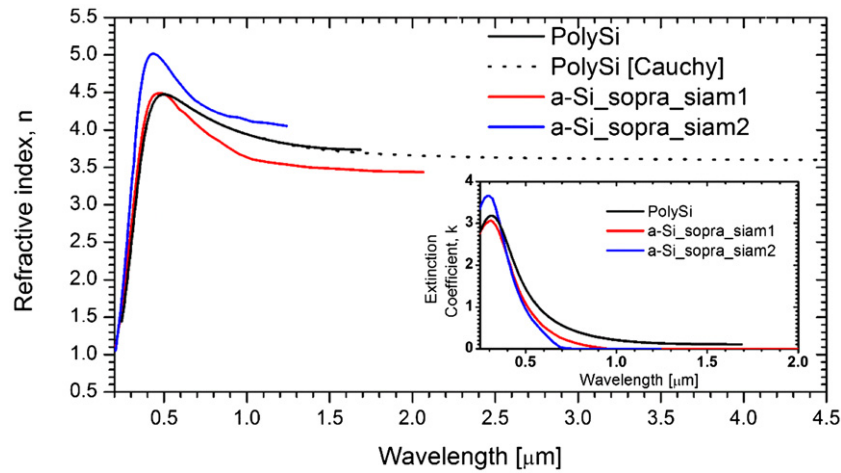


Figure 5. Optical constants for the sputtered polysilicon thin film analyzed by VASE. Optical constants of two different types of amorphous silicon are also included [28].

the wavelength of the transmitted beam. This yields a staircase-like lateral profile of the resonator width along the FP elements with constant step height. This becomes a taper with a constant taper angle for a large array of FP elements with a very narrow pitch between them. Therefore, the LVOF operates as a one-dimensional linear array of FP filters. Similar to the conventional FP resonators, the mirror reflectance determines the full-width half-maximum (FWHM) of the transmitted beam and hence the resolution of the spectrometer. However, the resolution of LVOFs is not only limited by the FWHM but also by the size of each detector unit [21].

Material selection is crucially important in optical filter design. The actual values of the refractive index of the high- and low- refractive index materials, which constitute the Bragg reflector, must be transparent in the desired wavelength range. In addition, they must have good optical contrast and be IC-compatible. Silicon and silicon-dioxide thin-films fulfill all of these requirements and were selected as high- and low- refractive index materials for LVOF design, respectively. A multi-layer out-of-band blocking filter was placed on top of the LVOF to block other transmission-orders of the LVOF. The thin-films were deposited using a commercial sputtering machine (FHR MS150, Germany). The sputtering conditions were tuned while the layers were characterized by variable-angle spectro-ellipsometric (VASE) measurements (J.A. Woollam M2000, Lincoln, NE, USA) to optimize the optical properties of the layers.

The Cauchy model (for dielectrics) [26], and various oscillator models such as the Lorentz model (for materials with band-gap in the optical range) [27] are usually used to analyze ellipsometry results. Here, we used the Cauchy model to extract the optical constants for silicon-dioxide, and Tauc-Lorentz for silicon thin-films. However, the ellipsometer used for the measurements operates only in the visible and short infrared region of the spectra, in the range of 250–1700 nm, and the acquired optical data does not cover the target spectral range (figure 5). Comparing the results with the literature shows that the optical constants of silicon thin-films are close to amorphous silicon. Since silicon is nonabsorbing in the mid-infrared and its refractive index is slowly decreasing with

Table 2. Layer thickness for IR LVOF in 3.0–4.5 μm wavelength range.

	#	Layer	Thickness (nm)
Mirror 1	1	SiO ₂	553.1
	2	Si	230.4
	3	SiO ₂	553.1
	4	Si	230.4
Resonator	5	SiO₂	900–1660
Mirror 2	6	Si	230.4
	7	SiO ₂	553.1
	8	Si	230.4
	9	SiO ₂	553.1
	10	Si	230.4
Out-of-band blocking filter	11	SiO ₂	175.5
	12	Si	147.5
	13	SiO ₂	350.9
	14	Si	147.5
	15	SiO ₂	350.9
	16	Si	147.5
	17	SiO ₂	350.9
	18	Si	73.7

wavelength, the optical constants of silicon can be modeled using the Cauchy equation in 1–1.7 μm wavelength range. Then, the wavelength range is extended up to 5 μm by extrapolating the Cauchy equation fitted over the ellipsometry data in 1–1.7 μm range (figure 5). For silicon-dioxide, the refractive index follows a decreasing trend and the extinction coefficient remains zero up to 2 μm in the literature [28]. The optical constants of silicon-dioxide that were extracted by the ellipsometer were extended in the infrared region up to 5 μm using the method above (figure 6). These values were then used in the optical thin-film simulations.

An LVOF was designed based on these optical constants for operation between 3.0 and 4.5 μm . Table 2 lists the thicknesses of the layers used in the design of this LVOF. This design employed two Bragg reflectors, one with four layers (#1–4) on top of the substrate and another one with five layers (#6–10) on top of the cavity. In between these two reflectors, a cavity with linearly varied thickness (#5) is placed.

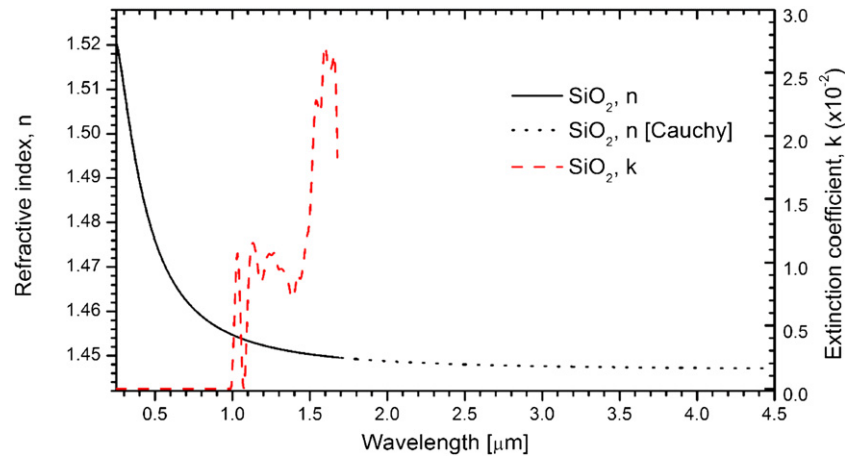


Figure 6. Optical constants for silicon-dioxide. (The absorption peaks around $1.5 \mu\text{m}$ corresponds to the presence of water vapor in the thin-film. The extinction coefficient was assumed to be zero over the operating range of LVOF.)

Figure 7 shows the expected transmission of the LVOFs designed, simulated using TFCalcTM software (Software Spectra, Portland, OR, USA), with the optical database built on the materials used in this filter and according to the layer thicknesses in table 2. This result revealed an expected transmission of more than 60% with a FWHM of less than 40 nm, which is equal to about 40 spectral channels in the range of operation.

4. LVOF fabrication

In 2012, Emadi *et al* [21] investigated an IC-compatible process-flow for fabricating visible LVOFs. In this study, we applied the same technique of using linearly variable distanced trenches to create a tapered cavity. However, to implement this approach for different wavelength ranges, other materials were selected considering both optical and cleanroom constraints.

The fabrication process flow is schematically presented in figure 8. At the beginning, the first four layers corresponding to the bottom Bragg reflector, and the thick resonator layer were sputtered on a silicon wafer. The SiO_2 thin-film layers were deposited by reactive RF sputtering and Si thin-films by RF sputtering (FHR MS150, Germany) alternately without breaking the vacuum. The thickness tolerances in the resonator layer do not influence the performance of the filter because of its linearity, though changing the thickness shifts all the peaks consistently. Hence, a larger thickness variation was targeted to include the intended range.

The blocking filter placed on top of the reflectors (#11–18) filters out the out-of-band transmission of the LVOF. The thickness of the resonator was set equal to the maximum cavity thickness in the optical design. In the next step, a $1.4 \mu\text{m}$ layer of positive photoresist (AZ9260) was spin-coated on the wafer, baked, and then patterned with a specially designed mask using a contact aligner (Karl Suss MA6/BA, Germany). This lithography step produces an array of trenches in the photoresist layer where each trench has a linearly variable distance from the neighboring trench, and hence the density of the trenches is different from one side of the filter to the other. This density defines the tapered angle of the resonator

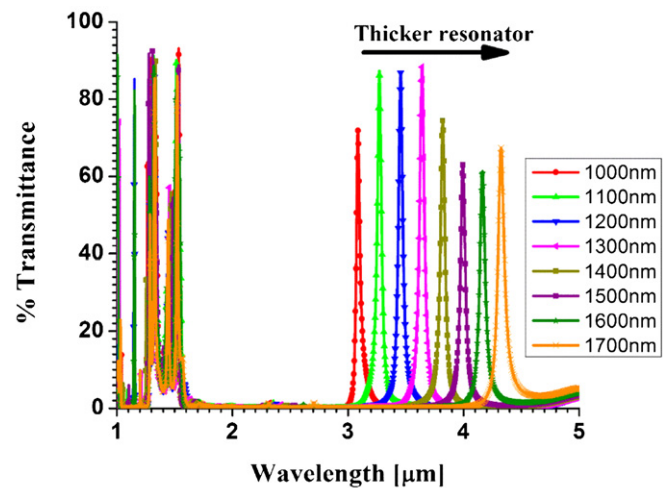


Figure 7. Expected transmission through the LVOF designed for 3–4.5 μm wavelength range while changing the thickness of the resonator layer (increasing the thickness shifts the peaks to higher wavelengths).

layer and hence the operating range and resolution of the filter. A chemical-thermal treatment smoothens the photoresist layer into a tapered structure (reflow) [22]. In this study the reflow was done in PGMEA vapor at 50°C followed by hard-baking at 100°C . An optimized plasma etching process in a CHF_3 and Ar mixture with a predefined photoresist-to-oxide etch ratio, transformed the tapered photoresist layer into the thick SiO_2 cavity layer. Finally, the remaining layers were sputtered to finalize the fabrication of the top Bragg-reflector and the out-of-band blocking filter.

5. Characterization and results

Based on the optical designs (table 2), two LVOF filters, both covering the same wavelength range but with different length were fabricated (8 and 3 mm active length). The long LVOF has a smaller slope and therefore, it comprises more channels. The longer LVOF has a higher resolving power, but at the expense of a larger chip area. The short LVOF on the other

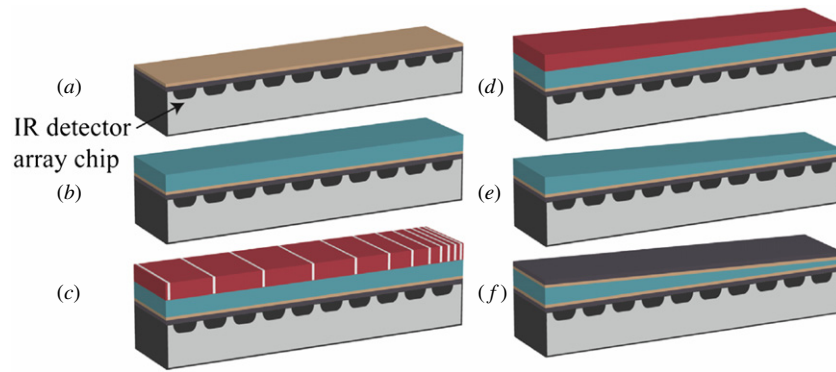


Figure 8. Fabrication process flow: (a) depositing the first Bragg reflector, (b) depositing the cavity layer, (c) patterning, (d) reflowing the photoresist, (e) transferring the tapered layer into oxide by dry etching, and (f) depositing the second multilayer Bragg reflector.

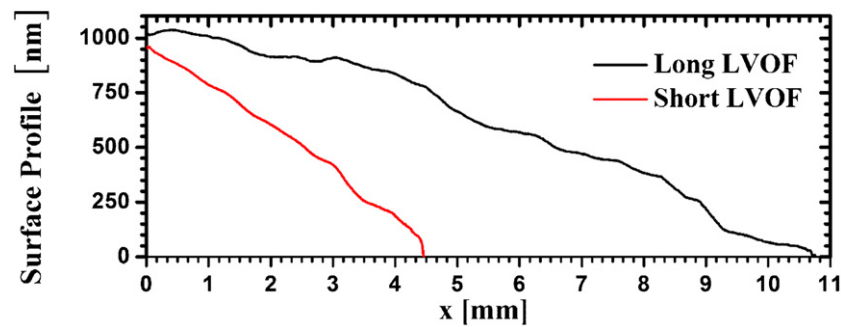


Figure 9. Profile of the 8 and 3 mm long LVOF including the margins on both sides.

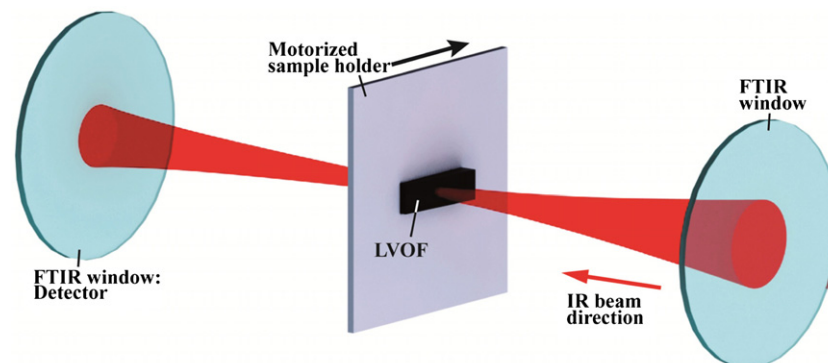


Figure 10. Schematic of the characterization setup.

hand, has a higher slope and fewer channels, which limits the resolving power.

Roughness is an important parameter that should be considered in optical absorption-based spectroscopy. An optical flatness worse than $\lambda/10$ degrades the optical performance. Therefore, considering the operating wavelength range (3.0–4.5 μm) in this particular filter design, the roughness should be less than 300 nm. The average roughness of both long and short LVOFs was measured by a 3D optical microscope (Bruker ContourGT-K1). Ten sampling areas (each 250 $\mu\text{m} \times 250 \mu\text{m}$) on each filter were analyzed, and the roughness average (R_a) was calculated as 102 nm for both. In addition to the optical roughness analysis, the profile of the LVOFs was also extracted. The results are shown in figure 9.

To characterize the filters, these were mounted on a motorized stage for positioning directly in the light path of an FTIR spectrometer (Bruker VERTEX70, Germany). The aperture size of the spectrometer, which is proportional to the spot size at the sample holder, can vary from 0.25 to 8 mm. The smallest aperture size (i.e. 250 μm) was selected to characterize the LVOFs. The filter was moved along its length and the transmission curve was measured at each step (figure 10). Figures 11 and 12 show the transmission curves obtained for the long and the short filters at different positions while moving the filter at 400 and 332 μm steps, respectively. The average FWHM obtained by this method was 100 nm and the transmittance was almost 40% for both filters. This proves that the filters are functional for the intended

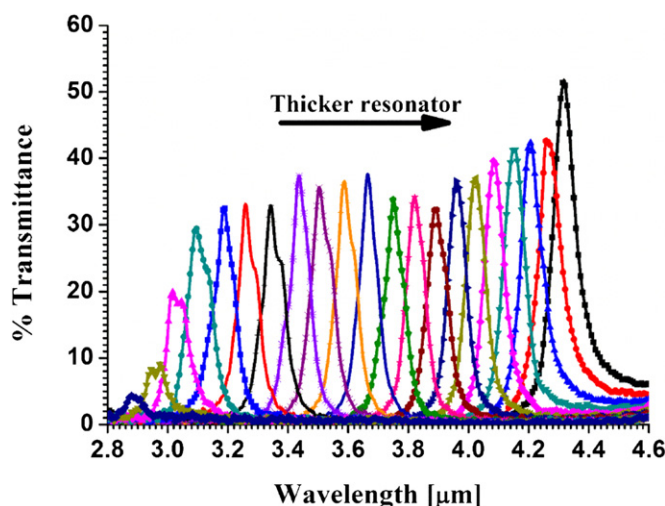


Figure 11. Measured transmission through an 8 mm long LVOF in infrared spectrum with 400 μm step size. Moving the LVOF shifts the transmitted peak from 3.0 to 4.4 μm .

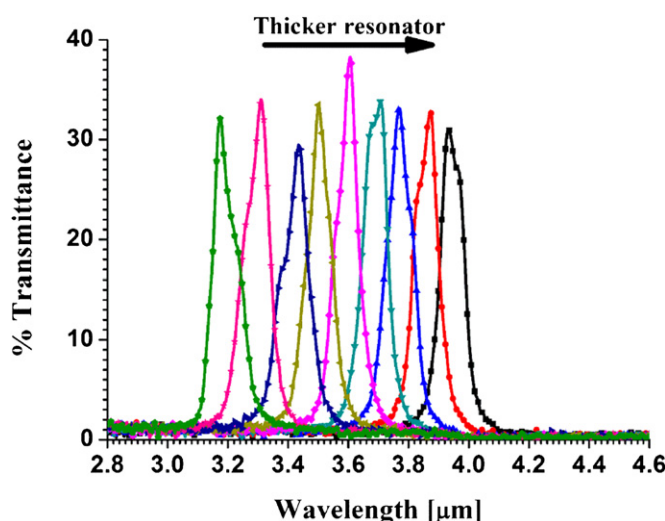


Figure 12. Measured transmission through a 3 mm long LVOF in infrared spectrum with 332 μm step size. Moving the LVOF shifts the transmitted peak from 3.0 to 4.0 μm .

application. The resolution can be further improved by post-processing algorithms (e.g. Kalman-filter) as suggested in [29].

6. Conclusion

This paper has presented the design, fabrication and characterization of infrared LVOF filters specially designed to measure the hydrocarbon content of combustible gases. Two different LVOFs with slope angles of 0.006° and 0.012° were fabricated. The micro-fabrication techniques were found to be effective for the fabrication of a functional IR micro-spectrometer. The transmission percentage and roughness average were measured with a commercial FTIR spectrometer and a 3D optical microscope, respectively. The measurement results show a FWHM resolution that is better than 100 nm and a roughness average (R_a) of 102 nm. Although the filter functions properly, this resolution does not meet all the

requirements of the intended application. The resolution is limited by the spot size as well as the wavelength range for which the filter is designed. In the actual micro-spectrometer, the spot size will be constrained by the pixel size of the detector. In characterization on the other hand, the aperture size of the instrument is the limiting factor. According to [21], the operating wavelength range (free spectral range: FSR) and FWHM are linearly proportional. Thus, by limiting the wavelength range, FWHM resolution can be improved.

The thickness tolerances increased the FWHM of the peaks, and also decreased the transmission level of the filter; however, due to the continuous nature of the LVOF, it did not influence the wavelength range transmitted through the filter. The on-going research is directed toward integrating the LVOF with arrays of thermal detectors on a micro-machined carrier. However, this study proved the feasibility of using LVOFs in micro-spectrometers for natural gas detection.

Acknowledgments

This work has been supported by the Dutch technology foundation STW under grant DEL.11476, and also by the Energy Delta Gas Research (EDGaR) program, which is co-financed by the Northern Netherlands Provinces, the European Fund for Regional Development, the Ministry of Economic Affairs and the province of Groningen. Devices were fabricated at MC2 of Chalmers University, Sweden.

References

- [1] Jurdik E, Turkstra J W, Otjes R, Groot T and Bakker F Sensors for new gases 2004 *Gasunie Research Report RT 2004.R. 0861*
- [2] de Graaf G, Bakker F and Wolffenbuttel R F 2011 Sensor platform for gas composition measurement *Proc. Eng.* **25** 1157–60
- [3] Dziuban J A et al 2004 Portable gas chromatograph with integrated components *Sensors Actuators A* **115** 318–30
- [4] Agilent Technologies 2013 Gas-chromatography www.chem.agilent.com
- [5] Brown A S, Milton M J, Cowper C J, Squire G D, Bremser W and Branch R W 2004 Analysis of natural gas by gas chromatography reduction of correlated uncertainties by normalisation *J. Chromatogr. A* **1040** 215–25
- [6] Debeda H, Dulau L, Dondon P, Menil F, Lucat C and Massok P 1997 Development of a reliable methane detector *Sensors Actuators B* **44** 248–56
- [7] Jones M G and Nevell T G 1989 The detection of hydrogen using catalytic flammable-gas sensors *Sensors Actuators* **16** 215–24
- [8] Azad A M, Akbar S A, Mhaisalkar S G, Birkefeld L D and Goto K S 1992 Solid-state gas sensors—a review *J. Electrochem. Soc.* **139** 3690–704
- [9] Korotcenkov G, Han S D and Stetter J R 2009 Review of electrochemical hydrogen sensors *Chem. Rev.* **109** 1402–33
- [10] Rahmouni C, Tazerout M and Corre O L 2003 Determination of the combustion properties of natural gases by pseudo-constituents *Fuel* **82** 1399–409
- [11] Hodgkinson J and Tatam R P 2013 Optical gas sensing: a review *Meas. Sci. Technol.* **24** 12004
- [12] Dias R A, de Graaf G, Wolffenbuttel R F and Rocha L A 2013 Gas viscosity MEMS sensor based on pull-in *17th Int. Conf.*

- on *Solid-State Sensors, Actuators and Microsystems (Barcelona, 2013)* pp 980–3
- [13] Andrews M K and Harris P D 1995 Damping and gas viscosity measurements using a microstructure *Sensors Actuators A* **49** 103–8
- [14] de Graaf G and Wolffenbuttel R F 2012 Surface-micromachined thermal conductivity detectors for gas sensing *Proc. IEEE Int. Instrumentation and Measurement Technology Conf.* pp 1861–4
- [15] Simon I and Arndt M 2002 Thermal and gas-sensing properties of a micromachined thermal conductivity sensor for the detection of hydrogen in automotive applications *Sensors Actuators A* **97–8** 104–8
- [16] Wolffenbuttel R F 2005 MEMS-based optical mini- and microspectrometers for the visible and infrared spectral range *J. Micromech. Microeng.* **15** S145–52
- [17] Rubio R et al 2007 Non-selective NDIR array for gas detection *Sensors Actuators B* **127** 69–73
- [18] Fonseca L et al 2009 Qualitative and quantitative substance discrimination using a CMOS compatible non-specific NDIR microarray *Sensors Actuators B* **141** 396–403
- [19] Rubio R et al 2006 Exploration of the metrological performance of a gas detector based on an array of unspecific infrared filters *Sensors Actuators B* **116** 183–91
- [20] Schuler L P, Milne J S, Dell J M and Faraone L 2009 MEMS-based microspectrometer technologies for NIR and MIR wavelengths *J. Phys. D: Appl. Phys.* **42** 133001
- [21] Emadi A, Wu H, de Graaf G and Wolffenbuttel R 2012 Design and implementation of a sub-nm resolution microspectrometer based on a linear-variable optical filter *Opt. Express* **20** 489–507
- [22] Emadi A, Wu H, Grabarnik S, de Graaf G and Wolffenbuttel R F 2009 Vertically tapered layers for optical applications fabricated using resist reflow *J. Micromech. Microeng.* **19** 074014
- [23] Emadi A 2010 Linear-variable optical filters for microspectrometer application *PhD Dissertation* Technical University of Delft
- [24] Linstrom P J and Mallard W G 2001 The NIST Chemistry WebBook: a chemical data resource on the internet *J. Chem. Eng. Data* **46** 1059–63
- [25] Tkachenko N V 2006 *Optical Spectroscopy: Methods and Instrumentations* (New York: Elsevier)
- [26] Tompkins H and McGahan W 1999 *Spectroscopic Ellipsometry and Reflectometry* (New York: Wiley)
- [27] Jellison Jr G and Modine F 1996 Parameterization of the optical functions of amorphous materials in the interband region *Appl. Phys. Lett.* **69** 371–3
- [28] Polyanskiy M N 2014 Refractive index database <http://refractiveindex.info>
- [29] Massicotte D, Morawski R Z and Barwicz A 1997 Kalman-filter-based algorithms of spectrometric data correction: part I. An iterative algorithm of deconvolution *IEEE Trans. Instrum. Meas.* **46** 678–84